Article

Aristolochene Synthase: Mechanistic Analysis of Active Site Residues by Site-Directed Mutagenesis

Brunella Felicetti, and David E. Cane

J. Am. Chem. Soc., **2004**, 126 (23), 7212-7221• DOI: 10.1021/ja0499593 • Publication Date (Web): 21 May 2004

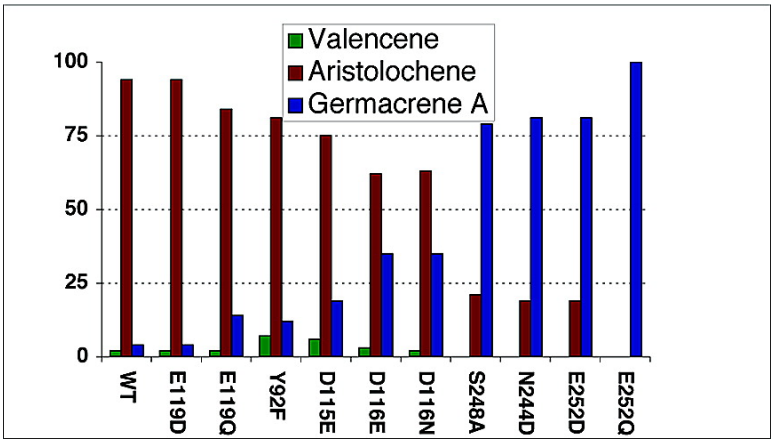

More About This Article

Additional resources and features associated with this article are available within the HTML version:

- Supporting Information
- Links to the 4 articles that cite this article, as of the time of this article download
- Access to high resolution figures
- Links to articles and content related to this article
- Copyright permission to reproduce figures and/or text from this article

View the Full Text HTML

J|A|C|S
ARTICLES
Published on Web 05/21/2004

Aristolochene Synthase: Mechanistic Analysis of Active Site Residues by Site-Directed Mutagenesis

Brunella Felicetti and David E. Cane*

Contribution from the Department of Chemistry, Box H, Brown University, Providence, Rhode Island 02912-9108

Received January 3, 2004; E-mail: David_Cane@brown.edu

Abstract: Incubation of farnesyl diphosphate (**1**) with *Penicillium roqueforti* aristolochene synthase yielded (+)-aristolochene (**4**), accompanied by minor quantities of the proposed intermediate (*S*)-(−)germacrene A (**2**) and the side-product (−)-valencene (**5**) in a 94:4:2 ratio. By contrast, the closely related aristolochene synthase from *Aspergillus terreus* cyclized farnesyl diphosphate only to (+)-aristolochene (**4**). Site-directed mutagenesis of amino acid residues in two highly conserved Mg^{2+}-binding domains led in most cases to reductions in both k_{cat} and k_{cat}/K_m as well as increases in the proportion of (*S*)-(−)germacrene A (**2**), with the E252Q mutant of the *P. roqueforti* aristolochene synthase producing only (−)-**2**. The *P. roqueforti* D115N, N244L, and S248A/E252D mutants were inactive, as was the *A. terreus* mutant E227Q. The *P. roqueforti* mutant Y92F displayed a 100-fold reduction in k_{cat} that was offset by a 50-fold decrease in K_m, resulting in a relatively minor 2-fold decrease in catalytic efficiency, k_{cat}/K_m. The finding that Y92F produced (+)-aristolochene (**4**) as 81% of the product, accompanied by 7% **5** and 12% **2**, rules out Tyr-92 as the active site Lewis acid that is responsible for protonation of the germacrene A intermediate in the formation of aristolochene (**4**).

Sesquiterpenes are among the most widely occurring and structurally diverse families of natural products. Compounds within this class display a broad range of physiological properties, including antibiotic, antitumor, phytotoxic and antifungal activities.[1] Sesquiterpenoids are produced by both marine and terrestrial plants as well as by numerous microorganisms, including fungi and actinomycetes.[2] More than 300 distinct sesquiterpene carbon skeletons have been identified to date and thousands of naturally occurring oxidized or otherwise modified derivatives have been isolated. Remarkably all sesquiterpenes are formed by cyclization of a common acyclic precursor, farnesyl diphosphate (FPP, **1**),[3] in a reaction catalyzed by enzymes known as sesquiterpene cyclases.[4] Each cyclase utilizes a common mechanism involving binding and ionization of the allylic diphosphate ester FPP (**1**) followed by a precise sequence of intramolecular electrophilic addition reactions and rearrangements. The diversity in product structure and stereochemistry can be explained in large part by the precise folding of the substrate FPP (**1**) at the sesquiterpene synthase active site.[4]

(+)-Aristolochene synthase is a fungal cyclase that catalyzes the divalent metal ion-dependent cyclization of farnesyl diphosphate (**1**) to the eremophilane sesquiterpene hydrocarbon (+)-aristolochene (**4**). Two distinct but closely related aristolochene synthases have been isolated to date, one from *Aspergillus terreus*[5] and the other *Penicillium roqueforti*.[6] On the basis of structural considerations (+)-aristolochene (**4**) is considered the likely parent hydrocarbon of several eremophilene toxins and bioregulators produced by a variety of filamentous fungi, including sporogen-AO 1,[7a] phomenone,[7b] and bipolaroxin.[7c] (+)-Aristolochene (**4**) is believed to serve as the precursor of PR-toxin, a mycotoxin produced by *P. roqueforti*.[7d] The enantiomer (−)-**4** has been isolated from a variety of plant sources, including *Aristolochia indica*[8a] and *Bixa orellana*,[8b] as well as from the defensive secretions of *Syntermes* soldier termites.[8c]

Aristolochene synthase from *P. roqueforti*, has been purified to homogeneity,[6] the structural gene has been cloned,[9] and the protein overexpressed in *Escherichia coli*.[10] The recombinant

(1) Lee, K.-H.; Hall, I. H.; Mar, E.-C.; Starnes, C. O.; El-Gebaly, S.; Waddell, T. G.; Hadgraft, R. I.; Ruffner, C. G.; Weidner, I. *Science* **1977**, *196*, 533−536. Anke, H. A.; Sterner, O. *Planta Med.* **1991**, *57*, 344−346. Habtemariam, S.; Gray, A. I.; Waterman, P. G. *J. Nat. Prod.* **1993**, *56*, 140−143. Kubo, I.; Himejima, M. *Experientia* **1992**, *48*, 1162−1164.
(2) Devon, T. K.; Scott, A. I. *Handbook of Naturally Occurring Compounds*; Academic Press: New York, 1972. Connolly, J. D.; Hill, R. A. *Dictionary of Terpenoids*; Chapman & Hall: London, 1992. Glasby, J. S. *Encyclopedia of Terpenoids*; Wiley: Chichester, 1982.
(3) Ruzicka, L. *Experientia* **1953**, *9*, 357−396.
(4) (a) Cane, D. E. *Acc. Chem. Res.* **1985**, *18*, 220−226. (b) Cane, D. E. *Chem. Rev.* **1990**, *90*, 1089−1103. (c) Cane, D. E. In *Isoprenoids Including Carotenoid and Steroids*; Cane, D. E., Ed. (Volume 2 in *Comprehensive Natural Products Chemistry*; Barton, D, Nakanishi, K., Meth-Cohn, O., Eds.); Pergamon Press: Oxford, 1999; pp 155−215.
(5) Cane, D. E.; Kang, I. *Arch. Biochem. Biophys.* **2000**, *376*, 354−364.
(6) Hohn, T. M.; Plattner, R. D. *Arch. Biochem. Biophys.* **1989**, *272*, 137−143.
(7) (a) Tanaka, S.; Wada, K.; Marumo, S.; Hattori, H. *Tetrahedron Lett.* **1984**, *25*, 5907−5910. (b) Riche, C.; Pascard-Billy, C.; Devys, M.; Gaudemer, A.; Barbier, M.; Bousquet, J. F. *Tetrahedron Lett.* **1974**, *32*, 2765−2766. (c) Sugawara, F.; Strobel, G.; Fisher, L. E.; Van Duyne, G. D.; Clardy, J. *Proc. Natl. Acad. Sci. U.S.A.* **1985**, *82*, 8291−8294. (d) Moreau, S.; Biguet, J.; Lablache-Combier, A.; Baert, F.; Foulon, M.; Delfosse, C. *Tetrahedron* **1980**, *36*, 2989−2997.
(8) (a) Govindachari, T. R.; Mohamed, P. A.; Parthasarathy, P. C. *Tetrahedron*, **1970**, *26*, 615. (b) Lawrence, B. M.; Hogg, J. W. *Phytochem.* **1973**, *12*, 2995. (c) Baker, R.; Cole, H. R.; Edwards, M.; Evans, D. A.; Howse, P. E.; Walmsley, S. *J. Chem. Ecol.* **1981**, *7*, 135.
(9) Proctor, R. H.; Hohn, T. M. *J. Biol. Chem.* **1993**, *268*, 4543−4548.
(10) Cane, D. E.; Wu, Z.; Proctor, R. H.; Hohn, T. M. *Arch. Biochem. Biophys.* **1993**, *304*, 415−419.

10.1021/ja0499593 CCC: $27.50

Scheme 1. Aristolochene Synthase Mechanism

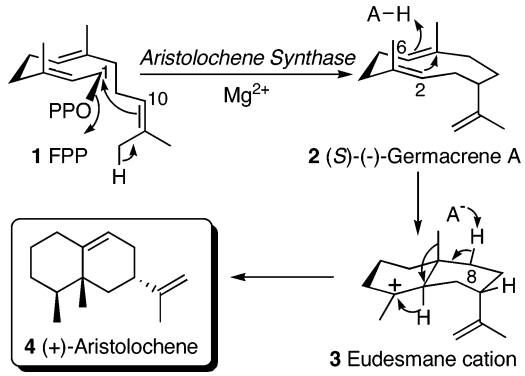

protein has a deduced composition of 342 amino acids corresponding to a M_D 39,191 Da. The *A. terreus* aristolochene synthase has also been purified to homogeneity and the corresponding structural gene has been cloned and overexpressed in *E. coli*.[5] The *A. terreus* protein has a deduced composition of 320 amino acids and is a monomer of M_D 36 480 Da. The *P. roqueforti* and *A. terreus* cyclases have 66% identity at the nucleic acid level and a 70% identity at the deduced amino acid level. Although neither of the two genes shows any significant overall sequence similarity to any protein in the protein- and DNA-databases, including known terpene synthases of both microbial and plant origin[5] the structure of *P. roqueforti* aristolochene synthase[11] shares a high level of structural homology with all other reported microbial and plant sesquiterpene synthases.[12]

Extensive mechanistic investigations using stereospecifically labeled derivatives of FPP (**1**) have provided strong support for an aristolochene synthase cyclization mechanism initiated by ionization of the allylic diphosphate ester to the corresponding allylic cation−pyrophosphate ion pair, followed by electrophilic attack at C-10 of the distal double bond and removal of a proton from the *cis*-C-12 methyl group, resulting in formation of the intermediate (*S*)-germacrene A (**2**) (Scheme 1).[13] The cyclization has been shown to take place with inversion of configuration at C-1 of FPP, as expected for a direct displacement mechanism.[13a] Once formed, the intermediate germacrene A (**2**) would be further cyclized by protonation at C-6 and intramolecular attack of the resultant carbocation on the C-2,3 bond to form the eudesmane cation (**3**). Successive 1,2-methyl migration and hydride shift followed by stereospecific deprotonation of H-8*si* (FPP numbering) will then result in the formation of (+)-aristolochene (**4**).[13b] The observed sequence of *anti*-migration and *syn*-deprotonation is readily explained by invoking a chair-boat conformation for the cyclizing FPP and intermediate germacrene A.

The proposed intermediate germacrene A is itself a commonly occurring sesquiterpene that has also been proposed as an intermediate in the cyclization of FPP (**1**) to a variety of bicyclic sesquiterpenes.[14] On the other hand, the formation of (*S*)-(−)-germacrene A (**2**) by aristolochene synthase had never previously been directly observed, although investigations with both mechanism based inhibitors[13c] and substrate analogues[13d] have provided substantial circumstantial evidence for its intermediacy in the formation of aristolochene. Interestingly, it has very recently been reported that *P. roqueforti* produces a set of sesquiterpenes of which the most abundant are (+)-aristolochene (**4**), valencene (**5**), α-selinene (**6**) and *β*-elemene (**7**), all of unspecified configuration (Scheme 2).[15a] Sporulated surface cultures of *P. roqueforti* also have been reported to produce (+)-aristolochene (**4**), valencene (**5**) and *β*-elemene (**7**) as the main volatile metabolites.[15b] Since it is well-known that *β*-elemene (**7**) and α-selinene (**6**) are readily formed from germacrene A (**2**) by thermal or acid-catalyzed rearrangement, respectively (Scheme 3),[16,17] detection of these sesquiterpenes in cultures of *P. roqueforti* producing (+)-aristolochene (**4**) is plausible but circumstantial evidence for the presence of germacrene A (**2**), itself possibly produced by aristolochene synthase. In like manner, valencene (**5**) could conceivably be formed by alternative deprotonation at C-6 of the penultimate

Scheme 2. Sesquiterpene Hydrocarbons Isolated from *P. Roqueforti*

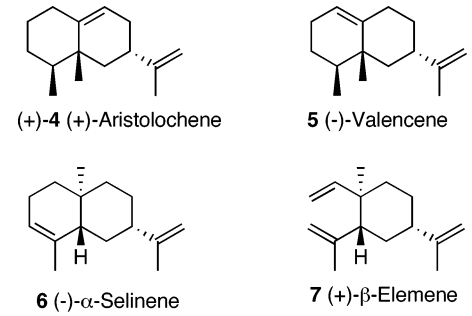

Scheme 3. Thermal and Acid-catalyzed Rearrangement of Germacrene A

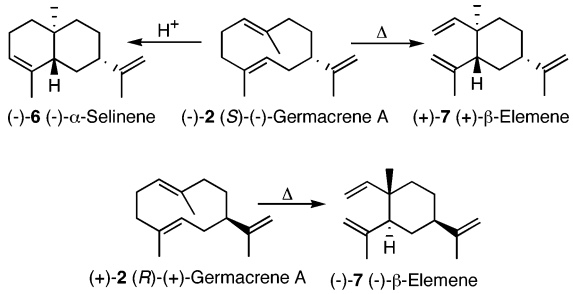

(11) Caruthers, J. M.; Kang, I.; Rynkiewicz, M. J.; Cane, D. E.; Christianson, D. W. *J. Biol. Chem.* **2000**, *275*, 25533−25539.

(12) (a) Lesburg, C. A.; Zhai, G.; Cane, D. E.; Christianson, D. W. *Science* **1997**, *277*, 1820−1824. (b) Rynkiewicz, M. J.; Cane, D. E.; Christianson, D. W. *Proc. Natl. Acad. Sci. U.S.A.* **2001**, *98*, 13 543−13 548. (c) Rynkiewicz, M. J.; Cane, D. E.; Christianson, D. W. *Biochemistry* **2002**, *41*, 1732−1741. (d) Starks, C. M.; Back, K.; Chappell, J.; Noel, J. P. *Science* **1997**, *277*, 1815−1820.

(13) (a) Cane, D. E.; Prabhakaran, P. C.; Salaski, E. J.; Harrison, P. H.; Noguchi, N.; Rawlings, B. J. *J. Am. Chem. Soc.* **1989**, *111*, 8914−8916. (b) Cane, D. E.; Prabhakaran, P. C.; Oliver, J. S.; McIlwaine, D. B. *J. Am. Chem. Soc.* **1990**, *112*, 3209−3210. (c) Cane, D. E.; Bryant, C. *J. Am. Chem. Soc.* **1994**, *116*, 12 063−12 064. (d) Cane, D. E.; Tsantrizos, Y. S. *J. Am. Chem. Soc.* **1996**, *118*, 10 037−10 040.

(14) (a) Whitehead, I. M.; Atkinson, A. L.; Threlfall, D. R. *Planta* **1990**, *182*, 81−88. (b) Back, K.; Chappell, J. *J. Biol. Chem.* **1995**, *270*, 7375−7381. (c) Rising, A. K.; Starks, C. M.; Noel, J. P.; Chappell, J. *J. Am. Chem. Soc.* **2000**, *122*, 1861−1866. (d) Munck, S. L.; Croteau, R. *Arch. Biochem. Biophys.* **1990**, *282*, 58−64. (e) Steele, C. L.; Crock, J.; Bohlmann, J.; Croteau, R. *J. Biol. Chem.* **1998**, *273*, 2078−2089.

(15) (a) Jelen, H. H. *J. Agric. Food Chem.* **2002**, *50*, 6569−6574. (b) Demyttenaere, J. C.; Adams, A.; Van Belleghem, K.; De Kimpe, N.; Konig, W. A.; Tkachev, A. V. *Phytochemistry* **2002**, *59*, 597−602.

(16) (a) de Kraker, J. W.; Franssen, M. C.; de Groot, A.; Konig, W. A.; Bouwmeester, H. J. *Plant Physiol.* **1998**, *117*, 1381−1392. (b) Weinheimer, A. J.; Youngblood, W. W.; Washecheck, P. H.; Harns, T. K. B.; Ciereszko, L. S. *Tetrahedron Lett.* **1970**, *7*, 497−500. (c) Bowers, W. S.; Nishino, C.; Montgomery, M. E.; Nault, L. R.; Nielson, M. W. *Science* **1977**, *196*, 680−681.

(17) Teisseire, P. J. In *Chemistry of Fragrant Substances*; VCH Publishers Inc.: New York, 1994; pp 193−289. de Kraker, J. W. *The Biosynthesis of Sesquiterpene Lactones in Chicory (Cichorium intybus L.) Roots, Doctoral thesis*, Department of Organic Chemistry; Wageningen University: Wageningen, 2002; pp 41−62.

Scheme 4. Formation of (+)-aristolochene (**4**) and (−)-valencene (**5**) by Alternative Deprotonation of the Common Intermediate **8**

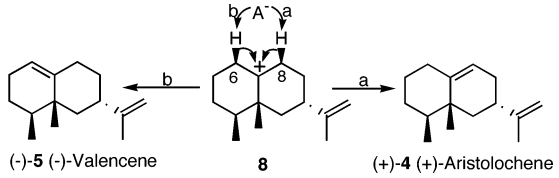

eremophilene cation (**8**) that normally yields (+)-aristolochene (**4**) (Scheme 4).

Important insights have come from analysis of the 2.5 Å crystal structure of recombinant *P. roqueforti* aristolochene synthase[11] which displays the all-helical class I α-helical terpenoid cyclase fold[12] in which 6 α-helices out of a total of 11 total surround a large, conical active site cleft approximately 15 Å wide by 20 Å deep (Figure 1). Remarkably, despite the absence of any significant amino acid sequence similarity, homologous structures are found in three additional sesquiterpene synthases: pentalenene synthase from the gram-positive bacterium *Streptomyces* UC5319,[12a] trichodiene synthase from the filamentous fungus *Fusarium sporotrichioides*,[12b,c] and epi-aristolochene synthase from the tobacco plant *Nicotiana tabacum*.[12d] Interestingly, the same terpenoid cyclase fold is also observed for avian farnesyl diphosphate synthase[18a] and for human squalene synthase.[18b] In all of these proteins, the sides and bottom of the active site cavity are predominately hydrophobic and contain a high proportion of aromatic residues. These amino acids confer an overall shape to the cavity, help to sequester the substrate and isolate it from the solvent, and define a unique contour that forms a template for the catalytically productive conformations of the substrate and intermediates. The upper region of the active site is usually somewhat hydrophilic in nature and contains polar and charged residues. Near the edge of the active site cavity of *P. roqueforti* arisolochene synthase is the universally conserved aspartate-rich motif[4c,18a,19] D^{115}DVLE and on the opposite wall is the other highly conserved amino acid sequence[5,12b,c] V^{242}V**N**DIY**S**YDK**E**, with the residues of the magnesium-binding triad indicated in bold (Figure 1). The crystal structures of *N. tabacum* epi-aristolochene synthase with a bound FPP analogue[12d] and of *F. sporotrichioides* trichodiene synthase complexed with the coproduct inorganic pyrophosphate[12b] have provided strong evidence that these two highly conserved motifs are together responsible for the binding of FPP through the chelation of three Mg^{2+} ions that in turn are complexed with the pyrophosphate moiety of the substrate. In each structure, two of these Mg^{2+} ions are liganded either directly or indirectly by two or more carboxylates of the aspartate-rich motif, whereas the third Mg^{2+} ion, which is complexed to the opposite face of the pyrophosphate moiety,

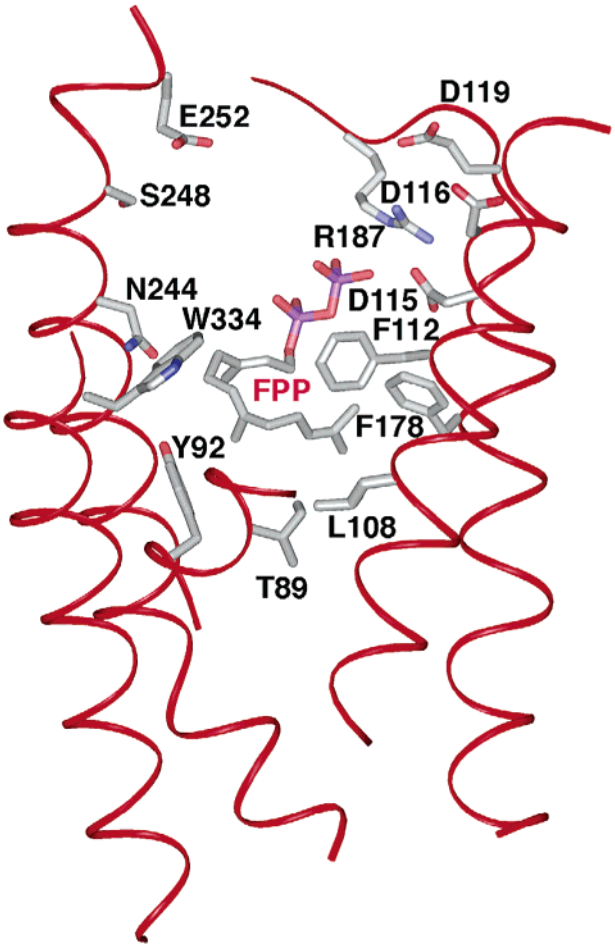

Figure 1. Active site of aristolochene synthase with model of bound FPP, showing key active site residues (ref 11).

is itself held in place by coordination to the side chains of the Asp/Asn, Ser, and Glu residues of the Mg^{2+}-binding triad. The pyrophosphate moiety of FPP (**1**) also forms hydrogen-bonds with basic Arg and Lys residues present at the top edge of the active site. The importance of the two conserved Mg^{2+}-binding motifs has been previously been probed by site-directed mutagenesis of several sesquiterpene synthases, including trichodiene synthase,[19d] pentalenene synthase,[20] δ-selinene synthase,[21] and γ-humulene synthase.[21]

We now describe site-directed mutagenesis experiments on aristolochene synthase from both *P. roqueforti* and *A. terreus* that substantiate the importance of the two conserved Mg^{2+}-binding motifs in each protein, provide direct evidence for the formation of the proposed intermediate (*S*)-(−)-germacrene A by both wild-type and mutant aristolochene synthases, and rule out the previously suggested role of Tyr-92 as an active site acid in the proton-initiated cyclization of the intermediate germacrene A.

Results

Recombinant wild-type aristolochene synthase from both *P. roqueforti* and *A. terreus* were each expressed and purified as previously described.[5,10] The k_{cat} (0.043 s^{-1}) and K_m (0.6 μM)

(18) (a) Tarshis, L. C.; Yan, M. J.; Poulter, C. D.; Sacchettini, J. C. *Biochemistry* **1994**, *33*, 10 871−10 877. (b) Pandit, J.; Danley, D. E.; Schulte, G. K.; Mazzalupo, S.; Pauly, T. A.; Hayward, C. M.; Hamanaka, E. S.; Thompson, J. F.; Harwood, H. J. *J. Biol. Chem.* **2000**, *275*, 30 610−30 617.
(19) (a) Croteau, R. B. In *Isoprenoids Including Carotenoids and Steroids*; Cane, D. E., Ed. (Volume 2 in *Comprehensive Natural Products Chemistry*; Barton, D, Nakanishi, K., Meth-Cohn, O., Eds.); Pergamon Press: Oxford, 1999; pp 97−153. (b) Tarshis, L. C.; Proteau, P. J.; Kellogg, B. A.; Sacchettini, J. C.; Poulter, C. D. *Proc. Natl. Acad. Sci. U.S.A.* **1996**, *93*, 15 018−15 203. (c) Ashby, M. N.; Edwards, P. A. *J. Biol. Chem.* **1990**, *265*, 13 157−13 164. (d) Cane, D. E.; Xue, Q.; Fitzsimons, B. C. *Biochemistry* **1996**, *35*, 12 369−12 376. (e) Marrero, P. F.; Poulter, C. D.; Edwards, P. A. *J. Biol. Chem.* **1992**, *267*, 21 873−21 878. (e) Song, L.; Poulter, C. D. *Proc. Natl. Acad. Sci. U.S.A.* **1994**, *91*, 3044−3048. (f) Joly, A.; Edwards, P. A. *J. Biol. Chem.* **1993**, *268*, 26 983−26 989. (g) Peters, R. J.; Croteau, R. B. *Proc. Natl. Acad. Sci. U.S.A.* **2002**, *99*, 580−584.
(20) Seemann, M.; Zhai, G.; de Kraker, J. W.; Paschall, C. M.; Christianson, D. W.; Cane, D. E. *J. Am. Chem. Soc.* **2002**, *124*, 7681−7689.
(21) Little, D. B.; Croteau, R. B. *Arch. Biochem. Biophys.* **2002**, *402*, 120−135.

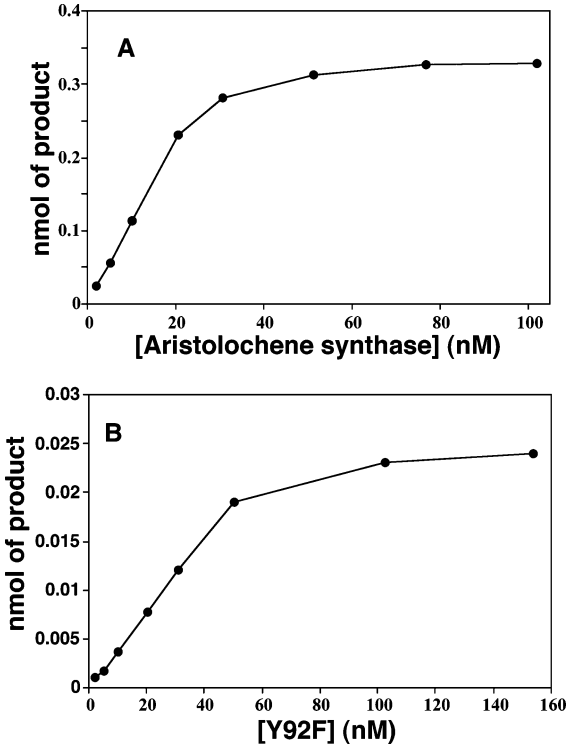

Figure 2. Concentration dependence of aristolochene synthase activity. Incubation for 10 min at variable protein concentration. (A) Wild-type *P. roqueforti* aristolochene synthase. (B) *P. roqueforti* Y92F mutant.

of the *P. roqueforti* cyclase were in good agreement with those previously reported[5] as were the k_{cat} (0.0173 s^{-1}) and K_m (0.13 μM) of the *A. terreus* enzyme.[10,22]

GC−MS analysis of the pentane extract of an incubation of FPP (**1**) with *A. terreus* aristolochene synthase showed a single product corresponding to (+)-aristolochene (**4**) (Figure 3). By contrast, the *P. roqueforti* enzyme produced two sesquiterpene hydrocarbons of *m/z* 204 in addition to the expected (+)-aristolochene (**4**), in relative proportions of 94 (**4**): 2 (**5**): 4 (**2**) (Figure 4). (−)-Valencene (**5**) was identified by direct GC-MS comparison with authentic (+)-valencene using a nonchiral stationary GC phase. When analyzed by chiral capillary GC, the enzymatically generated (−)-valencene (**5**) had a retention time of 51.04 min compared to a retention time of 51.84 min for (+)-valencene. (*S*)-(−)-Germacrene A (**2**) was first identified by capillary GC-MS comparison with a sample of (*R*)-(+)-germacrene A that was generated from FPP (**1**) by the W308F mutant of pentalenene synthase.[20] The absolute configuration of the enzymatically generated (*S*)-(−)-germacrene A (**2**) was established as previously described[16a] by means of its facile thermal Cope rearrangement to (+)-β-elemene (**7**) (Scheme 3).[16b] Using an injection port temperature of 250 °C, (−)-β-elemene ((−)-**7**) generated from (*R*)-(+)-germacrene A ((+)-**2**) and (+)-β-elemene ((+)-**7**) derived from the sample of **2** produced by aristolochene synthase (Scheme 3) had identical capillary GC-retention times on an Optima 1701 column and indistinguishable mass spectra. On the other hand the GC retention time (48.34 min) of (+)-β-elemene ((+)-**7**) derived from (*S*)-(−)-germacrene A ((−)-**2**) produced by aristolochene synthase clearly differed from that of (−)-β-elemene ((−)-**7**) (48.60 min) when the two compounds were analyzed by chiral capillary GC on FS-hydrodex-β-6TBDM.

Aspartate-Rich Domain. To investigate the functional role of the aspartate-rich domain in *P. roqueforti* aristochene synthase, appropriate D115E, D115N, D116E, D116N, E119D, and E119Q mutants were constructed by site-directed mutagenesis and expressed in *E. coli* BL21(DE3). Each recombinant mutant protein was purified to homogeneity. The *P. roqueforti* aristolochene synthase D115N mutant was completely inactive within the detection limits of the assay, which could have measured a reduction in k_{cat} of as much as a factor of 10^4. The steady-state kinetic parameters k_{cat} and K_m were determined for each purified mutant, and the product mixtures generated by each active mutant cyclase were analyzed by GC−MS (Table 2). In contrast to the lack of activity for the D115N mutant, replacement of Asp-115 with Glu (D115E) gave a mutant that retained substantial aristolochene synthase activity, displaying only a ~3-fold decrease in k_{cat} as well as a 4.5-fold increase in K_m, a net 12-fold decrease in catalytic efficiency, k_{cat}/K_m, compared to the wild-type enzyme. Replacement of Asp-115 with a glutamate also resulted in an increase in the proportion of both side products, (*S*)-(−)-germacrene A (**2**) and (−)-valencene (**5**), to 19% and 6%, respectively, of the total product mixture (Table 2).

The D116E mutant showed a 30-fold decrease in k_{cat} but only a 2-fold increase in K_m, resulting in a net 60-fold decrease in catalytic efficiency, while showing an 8-fold increase in the proportion of (*S*)-(−)-germacrene A (**2**) compared to the wild-type enzyme. Similarly the D116N mutant displayed a 20-fold reduction in k_{cat} and 3-fold increase in K_m, with a product distribution that was essentially identical to that obtained from the D116E mutant. By contrast, the E119D mutant did not display significant changes in either steady-state kinetic parameters (4-fold decrease in k_{cat} and 2-fold decrease in K_m) or in product distribution compared to the wild-type (Table 2). Although the replacement of Glu-119 by glutamine (E119Q) caused a 10-fold decrease in k_{cat} and a 4-fold decrease in K_m, with little net change in catalytic efficiency, the proportion of germacrene A (**2**) generated by the E119Q mutant increased to 14% of the total mixture.

Mg^{2+}-Binding Triad. To probe the role of the three putative Mg^{2+}-binding residues[12] in the conserved V^{242}V**N**DIY**S**YDK**E** domain of *P. roqueforti* aristolochene synthase, the N244L, N244D, S248A, E252D, and E252Q mutants, as well as the S248A/E252Q double mutant were each expressed in *E. coli* BL21(DE3) and purified to homogeneity. Both the N244L mutant and the double mutant S248A/E252D were completely inactive, within the detection limits of the assay. Aristolochene synthase activity was retained, however, when Asn-244 was replaced with aspartate (N244D), albeit with a k_{cat} that was reduced 350-fold compared to the wild-type and a K_m that was 6-fold higher, corresponding to a nearly 2000-fold decrease in k_{cat}/K_m (Table 2). The N244D mutant also exhibited a dramatic

(22) As previously reported, the activity of *P. roqueforti* aristolochene synthase is a simple linear function of protein concentration only within a specific concentration range.[10] The activity of wild-type aristolochene synthase was linearly proportional to protein concentration only up to 20 nM, after which the measured activity per mg protein decreased, with negligible increase in total activity above 60 nM protein (Figure 2A, Table 1). Similar behavior was also observed for the *A. terreus* aristolochene synthase, which displayed nonlinear dependence on protein concentration above 27 nM protein. To allow meaningful comparisons of steady state kinetic parameters, therefore, we first determined the concentration dependence of aristolochene synthase activity for all mutants prepared in this study. (Table 1) Kinetic assays of each mutant were then carried out only at protein concentrations within the experimentally established linear range.

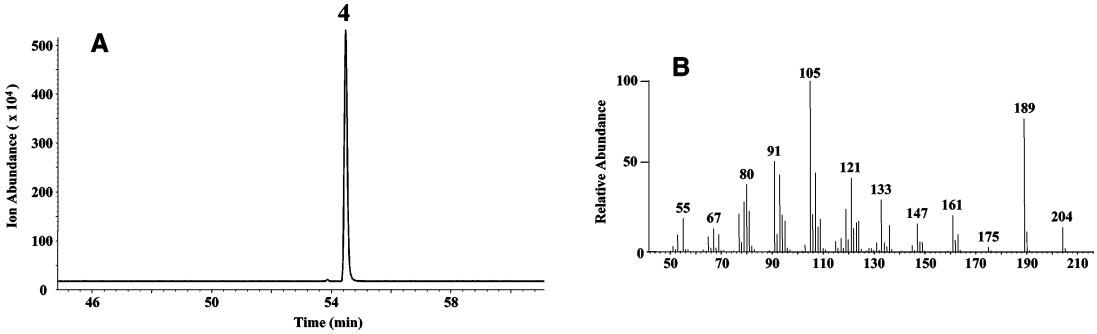

Figure 3. (A) GC−MS total ion chromatogram of *A. terreus* wild-type aristolochene synthase product. (B) Mass spectrum of (+)-aristolochene (**4**)

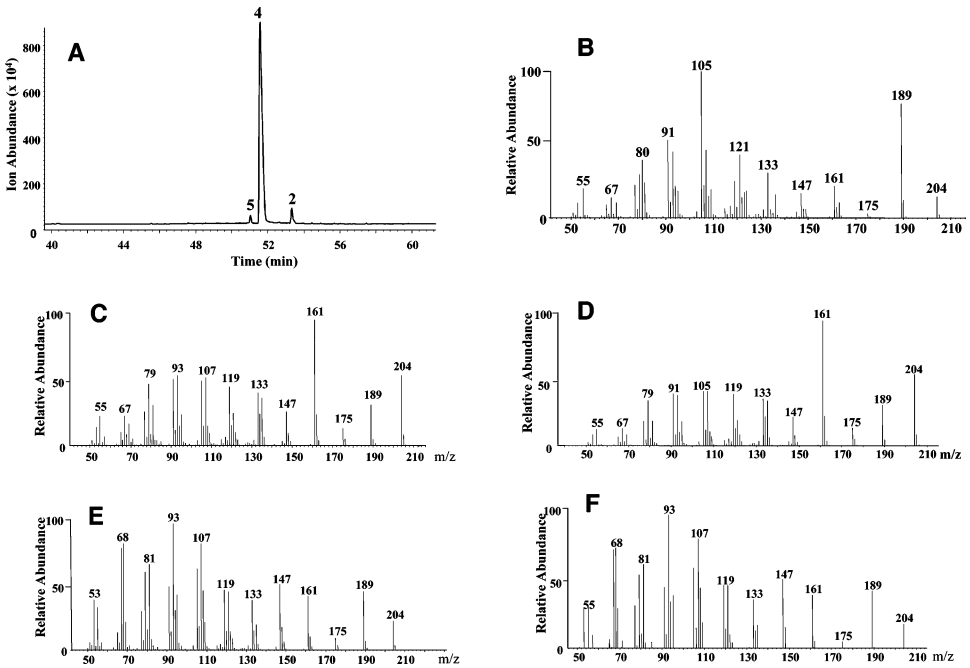

Figure 4. (A) GC−MS total ion chromatogram of *P. roqueforti* wild-type aristolochene synthase product mixture. (B) Mass spectrum of enzymatically generated (+)-aristolochene (**4**). (C) enzymatically generated (−)-valencene ((−)-**5**). (D) (+)-valencene ((+)-**5**). (E) enzymatically generated (*S*)-(−)-germacrene A ((−)-**2**). (F) (*R*)-(+)-germacrene A ((+)-**2**).

Table 1. Aristolochene Synthase, Wild-Type and Mutants: Concentration Range for Linear Dependence of Activity on Protein Concentration

protein	concentration range (nM)
P. roqueforti WT[a,b]	2−20
Y92F[b]	2−50
D115E[c]	2−160
D116E[c]	2−410
D116N[d]	2−510
E119D[d]	2−290
E119Q[d]	2−550
N244D[d]	2−510
S248A[e]	2−410
E252D[c]	2−410
E252Q[d]	2−520
A. terreus WT	0.9−27
AT-N219D	0.9−410
AT-E227D	0.9−410

[a] WT, wild-type. [b] 2 μM FPP, specific activity 44 μCi/μmol. [c] 10 μM FPP, specific activity 44 μCi/μmol. [d] 20 μM FPP, specific activity 44 μCi/μmol. [e] 4 μM FPP, specific activity 170 μCi/μmol.

shift in product distribution, with (*S*)-(−)-germacrene A (**2**) constituting 81% of the pentane-extractable products and (+)-aristolochene (**4**) making up the remaining 19% of the product mixture, no (−)-valencene (**5**) being detected (Table 2). The E252D and S248A mutants of *P. roqueforti* aristolochene synthase displayed more modest changes in steady-state kinetic parameters compared to the N244D mutant. Both showed a ca. 30-fold decrease in k_{cat} and a 300-fold decrease in k_{cat}/K_m compared to wild-type. On the other hand, the resulting product mixtures were almost identical to that produced by N244D, with (*S*)-(−)-germacrene A (**2**) the major product of the cyclization. Interestingly, the E252Q mutant displayed a 200-fold reduction in k_{cat} and a nearly 3500-fold reduction in k_{cat}/K_m. Most importantly, this mutant generated almost exclusively (*S*)-(−)-germacrene A (**2**) from FPP (**1**), with <0.1% (+)-aristolochene (**4**) and no detectable valencene (**5**) (See Supporting Information).

Although the structure of the *A. terreus* aristolochene synthase has not yet been solved experimentally, based on the high level of sequence similarity a working structural model was generated using the Swiss Protein Modeler and the *P. roqueforti* structure as a template. (Figure 5) Although such models are tentative, they can serve as useful guide to structure comparisons and as a source of further experiments, especially for proteins of high sequence identity. This model indicates that most of the amino

Table 2. Aristolochene Synthase Mutants: Kinetic Parameters and Product Ratios

protein	steady-state kinetic parameters			proportion of sesquiterpenes (%)		
	k_{cat} (10^{-3} s^{-1})	K_m (μM)	k_{cat}/K_m (s^{-1} M^{-1})	aristolochene (**4**)	valencene (**5**)	germacrene A (**2**)
P. roqueforti WT	43 ± 2	0.6 ± 0.1	7.2×10^4	94	2	4
D115E	16.2 ± 0.4	2.7 ± 0.2	6.0×10^3	75	6	19
D115N			inactive			
D116E	1.30 ± 0.05	1.10 ± 0.13	1.2×10^3	62	3	35
D116N	2.2 ± 0.1	1.5 ± 0.1	1.5×10^3	63	2	35
E119D	9.7 ± 0.2	0.32 ± 0.02	3.0×10^4	94	2	4
E119Q	4.8 ± 0.1	0.15 ± 0.02	3.2×10^4	84	2	14
N244L			inactive			
N244D	0.120 ± 0.003	3.3 ± 0.2	36.4	19	ND	81
S248A	1.30 ± 0.04	5.5 ± 0.4	2.4×10^2	21	ND*	79
E252D	2.20 ± 0.09	3.4 ± 0.4	6.5×10^2	19	ND	81
E252Q	0.22 ± 0.01	10.1 ± 0.7	21.8	ND	ND	100
S248A/E252D			inactive			
Y92F	0.40 ± 0.02	0.012 ± 0.002	3.4×10^4	81	7	12
A. terreus WT	17.3 ± 0.7	0.13 ± 0.01	1.3×10^5	100	ND	ND
AT-N219D	0.076 ± 0.004	3.9 ± 0.5	19.5	44	ND	56
AT-E227D	1.6 ± 0.1	1.4 ± 0.2	1.1×10^3	26	ND	74
AT-E227Q			inactive			

*WT, wild type; ND, not detected.

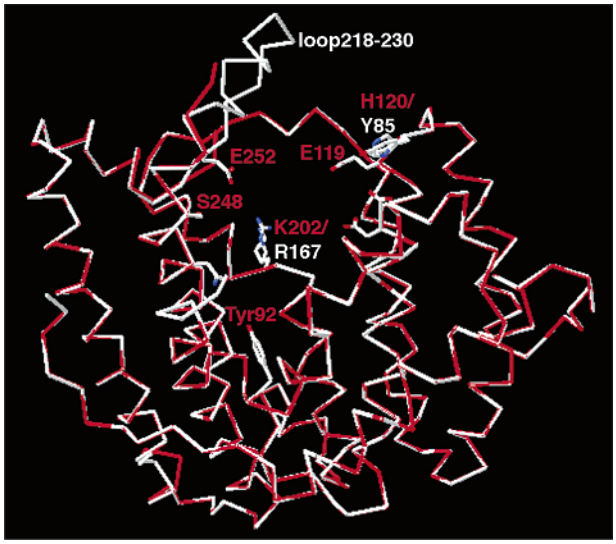

Figure 5. Comparison of Chain B of *P. roqueforti* aristolochene synthase (red) (PDB 1DI1B) with the structure of *A. terreus* aristolochene synthase (white) (Genbank Accession Number AF198360), calculated using the Swiss Modeler Program and displayed using the Swiss Protein Database Viewer (v 3.7).[32] Superposition of the two protein backbones gave a calculated RMSD for 1152 backbone atoms of 1.22 Å. Residues labeled in red are for the *P. roqueforti* protein and those in white are for the *A. terreus* enzyme. Selected residues labeled only in red are identical in both structures (although they have different residue numbers.) E119 is part of the conserved aspartate-rich motif DDXX**E**. E252 is part of the conserved triad NDXXSXXX**E**.

acids surrounding the active site are highly conserved in the two proteins, in accord with the fact that they both catalyze the cyclization of FPP (**1**) to (+)-aristolochene (**4**). In particular, the highly conserved aspartate-rich motifs (D^{90}DLLE for the *A. terreus* synthase and D^{115}DVLE for the *P. roqueforti* cyclase) and the magnesium-binding triads (N^{219}DIYSYEKE for the *A. terreus* synthase and N^{244}DIYSYDKE for the *P. roqueforti* synthase) are present at analogous positions in each cyclase, at the upper edges of the active site pocket. We therefore constructed a limited set of mutants of the *A. terreus* aristolochene synthase, targeting two of the residues of the magnesium-binding triad **N**^{219}DIY**S**YEK**E**. Accordingly, Asn-219 was replaced by an aspartate (*AT*-N219D) and Glu-227 was replaced by either an aspartate or a glutamine (*AT*-E227D, *AT*-E227Q). Each protein was overexpressed and purified as previously described.[5] The *AT*-E227Q mutant was inactive, whereas the *AT*-E227D mutant behaved similarly to the corresponding *P. roqueforti* E252D mutant, with (*S*)-(−)-germacrene A (**2**) being the major cyclization product. The *AT*-N219D mutant also was similar to the N244D mutant of *P. roqueforti* aristolochene synthase in kinetic properties, with a ~200-fold decrease in k_{cat} and a net ~6600-fold decrease in k_{cat}/K_m, and in product distribution, giving rise to a 56:44 mixture of (*S*)-(−)-germacrene A (**2**) and (+)-aristolochene (**4**) (Table 2).

Role of Tyr-92. The identity of the Lewis acid species in aristolochene synthase and mechanistically related enzymes responsible for protonation of the intermediate germacrene A (**2**) has been the object of considerable speculation and experimentation. Chappell and Noel have reported that replacement of Tyr-520 of 5-epi-aristolochene synthase by a phenylalanine abolishes formation of epi-aristolochene and results in the exclusive formation of germacrene A by this mutant, leading them to propose that Tyr-520 might correspond to the Lewis acid that protonates this intermediate in the cyclization of FPP to epi-aristolochene.[14c] Our previous analysis of the active site of *P. roqueforti* aristolochene synthase led also us to suggest that Tyr-92 might be suitably positioned to protonate the intermediate (*S*)-(−)-germacrene A.[11] To investigate the functional role of this residue, we therefore constructed the Y92F mutant of *P. roqueforti* aristolochene synthase by site-directed mutagenesis. Although the Y92F mutant exhibited a 100-fold decrease in k_{cat}, this reduced turnover number was offset by a compensating 50-fold decrease in K_m, resulting in substantially no net change in observed catalytic efficiency, k_{cat}/K_m, compared to the wild-type aristolochene synthase.[23] More significantly, this mutant produced (+)-aristolochene as the major product (81%), with only a modest increase in the relative proportions of both (*S*)-(−)-germacrene A (**2**) (12%) and (−)-valencene (**5**) (7%) compared to the wild-type cyclase.

(23) The activity of the Y92F mutant was found to be a simple linear function of protein concentration only up to 50 nM (Figure 2B, Table 1), with only minor increases in total cyclase activity above 80 nM mutant protein.

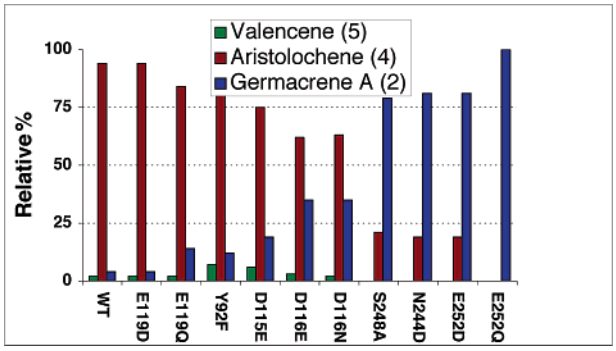

Figure 6. Product distribution of *P. roqueforti* aristolochene synthase mutants.

Discussion

Formation of (−)-Germacrene A (2) and (−)-Valencene (5). Cultures of *P. roqueforti* have been reported to accumulate, in addition to aristolochene, small quantities of valencene, of unspecified configuration, and a variety of sesquiterpenes readily derived from germacrene A.[15] Allemann has recently reported that wild-type recombinant *P. roqueforti* aristolochene synthase generates small quantities of both valencene (**5**) and germacrene (**2**), again of unspecified configuration.[24] We have now independently established that *P. roqueforti* aristolochene synthase converts FPP to a 94:2:4 mixture of (+)-aristolochene (**4**), (−)-valencene (**5**), and (*S*)-(−)-germacrene A (**2**) and rigorously determined the absolute configuration of each product. Interestingly, the very closely related *A. terreus* enzyme generates (+)-aristolochene as the sole sesquiterpene hydrocarbon product. Although the formation of product mixtures is unusual for microbial terpene synthases, it is very common for plant terpene synthases. Two particularly striking examples are those of γ-humulene synthase and δ-selinene synthase, which cyclize FPP to 52 and 34 different sesquiterpenes, respectively.[14e]

The absolute configuration of the (*S*)-(−)-germacrene A (**2**) produced by *P. roqueforti* aristolochene synthase is consistent with the well-supported absolute sense of folding of FPP (**1**) in the formation of (+)-aristolochene (**4**)[4b,13a,b] and therefore supports the intermediacy of **2** previously inferred from experiments with substrate analogues[13d] and mechanism-based inhibitors.[13c] The observed formation of a small proportion of (S)-(−)-germacrene A (**2**) from FPP is apparently due to its premature release from the active site before it can be reprotonated and further converted to the eudesmane cation. The absolute configuration of the enzymatically generated (−)-valencene ((−)-**5**) is also consistent with the configuration of the major product, (+)-aristolochene (**4**). This side product arises by deprotonation at C-6 instead of C-8 in the penultimate cation intermediate **8** (Scheme 4). In principle, the same active site base could remove a proton from either position, resulting in the formation of minor amounts of (−)-valencene (**5**) along with the favored product, (+)-aristolochene (**4**).

Mutations in the two Mg^{2+}-binding domains of each of the two aristolochene synthases substantially affected the observed distribution of products (Table 2, Figure 6). The various mutants in the aspartate-rich region, **D**^{115}**D**VL**E**, of the *P. roqueforti* synthase release a greater proportion of the cyclization intermediate (*S*)-(−)-germacrene A (**2**) (14%-35%) compared to the wild-type (4%). By contrast, the fraction of the alternative deprotonation product, (−)-valencene (**5**) is generally unchanged, increasing from 2% to 6% only for the D115E mutant. More dramatic shifts in product distribution were observed for mutations in the residues of the Mg^{2+}-binding triads, N^{244}DIYSYDKE and N^{219}DIYSYEKE, of the *P. roqueforti* and *A. terreus* synthases, respectively, with the proportion of (−)-germacrene A (**2**) increasing to 55%-75% for the *A. terreus* N219D and E227D mutants, 80% for the three *P. roqueforti* N244D, S248A, and E252D mutants, and reaching 100% of total sesquiterpene for the *P. roqueforti* E252Q mutant. These increases in the percentage of prematurely released germacrene A (**2**) are associated, however, with substantial kinetic penalties, with degradations in the observed k_{cat}/K_m by factors from 100 to as much as 6500.

The formation of aberrant product mixtures resulting from mutations in the Mg^{2+}-binding domains is believed to be due to perturbations in the precise binding of the pyrophosphate moiety of the substrate FPP, with consequent mispositioning of the farnesyl chain as well as the derived carbocationic and neutral intermediates. Although there is no direct evidence that the essential Mg^{2+} cations are bound by aristolochene synthase at the two universally conserved Mg^{2+}-binding motifs, the crystal structure of the $SmCl_3$-derivative of *P. roqueforti* synthase shows a single Sm^{3+} ion bound to Asp-115.[11] Consistent with this model are the results of site-directed mutagenesis experiments with trichodiene synthase, in which replacement of Asp-100 of the aspartate-rich motif with glutamate resulted in a 22-fold reduction in observed k_{cat} and the formation of a mixture of five aberrant cyclization products, in addition to trichodiene.[19d] Similar results were also obtained for the D101E and D104E mutants of trichodiene synthase. The crystal structure of the D100E mutant of trichodiene synthase with bound inorganic pyrophosphate showed that only two of the usual three Mg^{2+} ions remains bound to the inorganic pyrophosphate, with one of the two Mg^{2+}-ions normally bound to the aspartate-rich domain of the wild-type cyclase no longer present, resulting in a shift in the position of the bound inorganic pyrophosphate.[12c] Most importantly the conformational changes associated with pyrophosphate binding by the wild-type trichodiene synthase were attenuated in the D100E mutant, resulting in a 12% increase in the included active site volume and a calculated decrease in the packing density of the substrate FPP (**1**) from 78% to 67%.[12b,c] The concomitant increases in spatial and conformational degrees of freedom for the mutant-bound substrate and derived reactive intermediates are thought to permit premature deprotonation of intermediates, resulting in formation of the observed aberrant products.

Kinetic Properties of Aristolochene Synthase Mutants. Four of the aristolochene synthase mutants were completely inactive, including one with a mutation in the aspartate-rich domain (D115N) and three involving the three residues of the Mg^{2+}-binding triad: N244L, the double mutant S248A/E252D and the *A. terreus* mutant E227Q. The homologous N219L and N219A mutants of pentalenene synthase have also been found to be inactive.[20] Analysis of the crystal structure of the N219L mutant of pentalenene synthase revealed no significant changes in the shape of the active site or in protein structure compared

(24) (a) Calvert, M. J.; Ashton, P. R.; Allemann, R. K. *J. Am. Chem. Soc.* **2002**, *124*, 11 636−11 641. (b) Deligeorgopoulou, A.; Allemann, R. K. *Biochemistry* **2003**, *42*, 7741−7747. (c) Calvert, M. J.; Taylor, S. E.; Allemann, R. K. *Chem. Commun.* **2002**, 2384−2385.

to the wild-type enzyme, suggesting that the observed loss of cyclase activity involves disruption of a key interaction with the substrate.[20] Interestingly, the substitution of an alanine for Ser-248 of aristolochene synthase, a residue that is believed to coordinate to the same Mg^{2+} ion as Asn-244, did not abolish the aristolochene synthase activity, resulting instead in a 300-fold reduction in k_{cat}/K_m and a substantial increase in the proportion of germacrene A. Similarly, the replacement of Glu-252 of the *P. roqueforti* aristolochene synthase with an aspartate or a glutamine also did not cause complete loss of activity of the enzyme. Only the *P. roqueforti* double mutant, S248A/E252D, in which two Mg^{2+} coordination sites were perturbed, was found to be inactive. Although the corresponding E227D mutant of the *A. terreus* enzyme was also found to be inactive, these apparent differences may simply reflect the lower limits for the detection of reduced cyclase activity. In general, mutations in the Mg^{2+}-binding triad appeared to have more profound effects on both catalytic efficiency and product distribution than variants in the aspartate-rich motif, with changes in D119 having the smallest net effect.

Role of Tyr-92. The observation that (+)-aristolochene (**4**) is still the major product (81%) of the cyclization reaction catalyzed by the Y92F mutant of *P. roqueforti* aristolochene synthase, and that it is produced with basically the same k_{cat}/K_m, although at substantially lower k_{cat}, compared to the wild-type enzyme, definitively rules out Tyr-92 as the active site Lewis acid responsible for the protonation of the intermediate germacrene A (**2**).[25] Recent reports from other laboratories have also shed doubt on the original suggestion that Tyr-520 of epi-aristolochene synthase serves as the active site acid in the protonation-cyclization of germacrene A. For example, Tyr-520 and its hydrogen-bonded Asp-444 and Asp-525 are conserved in chicory germacrene A synthase, as well as in most of the other known germacrene A synthases.[26] The presence of these residues therefore cannot alone account for the formation of either germacrene A or epi-aristolochene as the end-product of their respective synthases. Furthermore, it has recently been reported that germacrene A is released from the active site of wild-type epi-aristolochene synthase when cyclizations are carried out at elevated pH.[27] Indeed, at pH > 8.8, germacrene A becomes the major product of cyclization of FPP (**1**) by epi-aristolochene synthase, indicating that the changes in the protonation state of the active site acid can suppress the normal protonation of the germacrene A intermediate. Interestingly, the Y520F mutant of epi-aristolochene synthase was also found to produce both epi-aristolochene and germacrene A, but the transition to exclusive production of germacrene A occurs at pH 7, lower than for the wild-type. The identity of the active site acids in the cyclization of FPP (**1**) to both (+)-aristolochene (**4**) and epi-aristolochene therefore still remains an open question. One attractive possibility is that a protonated water molecule might serve as the requisite Lewis acid but there is as yet no direct data yet available to support this possibility. The recent observation that the active site of bornyl diphosphate synthase contains a bound molecule of water is at least consistent with this hypothesis.[28] The identification of the active site acid of aristolochene synthase will no doubt require analysis of high-resolution crystal structures of protein with bound substrate or intermediates analogues.

Conclusions. Site-directed mutagenesis of aristolochene synthase from both *P. roqueforti* and *A. terreus* has provided strong support for the proposed intermediacy of (*S*)-(−)-germacrene A (**2**) in the conversion of FPP (**1**) to (+)-aristolochene (**4**). The effect of mutations in the two conserved Mg^{2+}-binding domains has reinforced earlier observations on the importance of residues in these two regions in binding and ionization of the pyrophosphate moiety of the FPP. The fact that the Tyr92Phe mutant of *P. roqueforti* aristolochene synthase produces aristolochene as the major (>80%) product, albeit at reduced rate, definitively rules out this residue as the active site Lewis acid directly responsible for the protonation and further cyclization of the germacrene A intermediate. The identity of the requisite active site bases and acids responsible for the various deprotonation and protonation steps in the cyclization cascade catalyzed by aristolochene synthase and other terpene cyclases remains to be established and is the subject of further investigation.

Experimental Section

Materials. Recombinant *P. roqueforti A. terreus* aristolochene synthases were obtained from *E. coli* XL1 Blue/pZWO4, *E. coli* XL1 Blue/pET11rASa, *E. coli* BL21(DE3)/pZWO4 and *E. coli* BL21(DE3)-pLysS/pET11rASa as previously described.[5,10] The QuikChange site-directed mutagenesis kit was purchased from Stratagene. Mutagenic and sequencing primers were purchased from Integrated DNA Technology, Inc. Competent cells of *E. coli* BL21(DE3), *E. coli* BL21(DE3)-pLysS and *E. coli* XL1-Blue were purchased from Stratagene. The QIAprep spin Miniprep plasmid purification kit was purchased from Qiagen. Culture media were obtained from Sigma. Isopropyl-thio-*D*-galactopyranoside (IPTG) was purchased from Gibco and β-mercaptoethanol was obtained from Sigma. Pre-swollen DE52 anion-exchange resin was from Whatman. The pre-packed methyl hydrophobic interaction column (methyl-HIC, 5 mL) was obtained from BioRad. The Resource Q anion exchange column was purchased from Pharmacia Biotech. Corp. Protein size marker was purchased from Bio-Rad. The Amicon-YM30 membranes and Centriprep YM-30 disposable ultrafiltration units were from Millipore. The Bradford protein assay reagent and the concentrated electrophoresis buffer were from Bio-Rad. [1-^{3}H]FPP (16.1 Ci/mmol) was purchased from New England Nuclear (NEN), DuPont. Unlabeled FPP (**4**) was synthesized following the procedure described in the literature.[29] Authentic (+)-valencene was

(25) Allemann et al.[24] have used the p ZWO4 aristolochene synthase expression plasmid obtained from our laboratory to generate the corresponding Y92F, Y92V, Y92C, and Y92A mutants. For the Y92F mutant, Allemann reported a 13-fold reduction in k_{cat} and a ~80-fold increase in K_m, resulting in a reported net ~1100-fold decrease in k_{cat}/K_m compared to the wild-type.[24a] The reported steady-state kinetic parameters were unfortunately determined at concentrations well above what turns out to be the maximum 50 nM protein concentration for linear dependence of Y92F activity (cf Table 1), thereby compromising their quantitative significance. On the basis of an observed increase in the proportion of germacrene A (28%), of unspecified configuration, the implausible suggestion was made that Tyr-92 must be the normal active site Lewis acid responsible for the cyclization of the germacrene A intermediate, although the major product isolated was still aristolochene. These workers also reported the isolation of the coproducts α-selinene (**6**), β-selinene, and selina-4,11-diene, none of which are detectable in our analysis of the same Y92F mutant (Table 2). The latter compounds are well-known artifacts of the acid-catalyzed rearrangement of germacrene A.[16,17,20] Rearrangement of germacrene A is easily avoided by chromatography over aluminum oxide instead of silica gel and the use of sodium sulfate in place of magnesium sulfate as drying agent.

(26) Bouwmeester, H. J.; Kodde, J.; Verstappen, F. W.; Altug, I. G.; de Kraker, J. W.; Wallaart, T. E. *Plant Physiol.* **2002**, *129*, 134−144.

(27) O'Maille, P.; Greenhagen, B.; Chappell, J.; Zhao, Y.; Coates, R. M.; Noel, J. Poster Presentation: *TEAS: A Closer Look at the Cyclization Cascade*; Terpnet 2003, Lexington, Kentucky, 2003.

(28) Whittington, D. A.; Wise, M. L.; Urbansky, M.; Coates, R. M.; Croteau, R. B.; Christianson, D. W. *Proc. Natl. Acad. Sci. U.S.A.* **2002**, *99*, 15 375−15 380.

(29) Cane, D. E.; Sohng, J. K.; Lamberson, C. R.; Rudnicki, S. M.; Wu, Z.; Lloyd, M. D.; Oliver, J. S.; Hubbard, B. R. *Biochemistry* **1994**, *33*, 5846−5857.

obtained from Fluka. (*R*)-(+)-germacrene A was prepared by incubation of FPP (**1**) with the W308F mutant of pentalenene synthase (plasmid pMSO4), as previously described.[20] All other reagents and buffer components used for protein purification and enzyme assay were of the highest quality commercially available.

General Methods. Standard recombinant DNA and protein manipulations were carried out according to published procedures.[30] PCR and restriction digestions were run in a MiniCycler thermocycler from MJ Research, equipped with a hot-bonnet. Aristolochene synthase mutants were generated with the QuikChange site-directed mutagenesis kit using the manufacturer's protocols. DNA sequencing was performed by the HHMI Biopolymer/Keck Foundation Biotechnology Resource Laboratory at the Yale University School of Medicine, New Haven (CT), using the dideoxy dye terminator method and automated fluorescence sequencing. Protein concentrations were determined by the Bradford method using commercial reagents (Bio-Rad) and bovine serum albumin (Sigma) as a calibration standard.[31] Liquid scintillation was performed on a Beckman Model LS-6500 liquid scintillation counter using Packard OmniFluor scintillation cocktail. Analysis of DNA and protein sequences as well as PCR primer design utilized the suite of programs in the GCG Sequence Analysis Package, version 10.0 (Unix), from Accelrys. The Insight II software package (Accelrys) was used to visualize and manipulate Protein Data Bank (PDB) files corresponding to the crystal structures of aristolochene synthase (accession code 1DI1) and that of aristolochene synthase complexed with FPP (**1**) (accession code 1F1P). A structural model of the *A. terreus* aristolochene synthase (Genbank accession number AF198360) was generated through the Swiss-Model website (http://swissmodel.expasy.org) using the structure of chain B of the *P. roqueforti* enzyme (1DI1B) as a template.[32] GC−MS analysis of enzymatic reaction products was performed using a HP-GCD series II GC−MS system equipped with either an Optima 1701 capillary GC column (14% cyanopropyl-phenyl/86% dimethyl polysiloxane) or a chiral capillary GC column (FS-hydrodex-β-6TBDM), both purchased from Macherey-Nagel. Both columns were 30 m in length with an internal diameter of 0.25 mm and 0.25 μm phase thickness.

Aristolochene Synthase Mutants. Aristolochene synthase mutants were prepared by PCR mutagenesis with the QuikChange site-directed mutagenesis kit according to the manufacturer's protocols, using as template plasmid DNA from pZW04, harboring the *P. roqueoforti* aristolochene synthase[10] or pET11rASa, harboring the *A. terreus* aristolochene synthase.[5] For the *P. roqueforti* double mutant, S248A/E252Q, the E252Q mutation was introduced using the plasmid pZWO4/S248A as the template for PCR. Plasmid pZWO4 was extracted from an overnight culture of *E. coli* XL1Blue/pZWO4 grown in Luria Bertani (LB) ampicillin (100 μg/mL) medium, and purified using the Miniprep plasmid purification kit. For each mutation the forward and the reverse mutagenenic primers consisted of two complementary oligonucleotides (25−45 nt) containing the desired mutation flanked by unmodified nucleotide sequences. Each primer was designed and purified according to the vendor's recommendations. Mutant plasmids isolated from overnight cultures of three separate colonies were purified by plasmid miniprep and the incorporation of the desired mutation was verified by DNA sequencing. One of the sequenced plasmids was then utilized to transform competent cells of the expression host strain *E. coli* BL21(DE3). From the resultant transformants, three single colonies were chosen and assayed by SDS-PAGE for aristolochene synthase production after IPTG induction. All of the colonies were found to overexpress the enzyme. The colony giving rise to the highest level of expression, as judged by SDS-PAGE, was then used for kinetic analysis and preparative scale incubations.

***P. roqueforti* Aristolochene Synthase.** Individual strains of *E. coli* BL21(DE3) harboring mutant plasmids for *P. roqueforti* aristolochene synthase were each grown overnight in 8 mL of LB medium containing 100 μg/mL ampicillin at 37 °C. The resulting culture (8 mL) was used to inoculate pre-warmed LB medium (800 mL, 100 μg/mL ampicillin) and the cells were grown at 30 °C to an OD_{600} of 1.0. Protein expression was then induced with 1 mM IPTG. Following 6 h of incubation at 30 °C (250 rpm) the cells were harvested by centrifugation (6000 × *g*, 25 min, 4 °C). The cell pellet was resuspended in 50 mL of cell lysis buffer (5 mM EDTA, 5 mM β-mercaptoethanol, 20 mM Tris pH 7.5) and recentrifuged (6000 × *g*, 25 min, 4 °C) to remove any remaining LB medium. The cells were then suspended in 50 mL of lysis buffer and broken by sonication (three cycles of 10 min each, 30% power range, 50% duty cycle) in an ice water bath. The pellet was then resuspended in the same buffer and recentrifuged to remove traces of soluble protein. The subsequent solubilization and purification of the mutant proteins were performed as previously described for wild-type *P. roqueforti* aristolochene synthase.[11] Fractions containing pure enzyme were identified by SDS-PAGE, combined, and concentrated to a final volume of 2.5 mL using an Amicon ultrafiltration apparatus equipped with a YM-30 filter. The final enzyme purity was greater than 90% as judged by SDS-PAGE analysis. The concentrated protein was dialyzed against Buffer T (20 mM Tris pH 7.5, 15% glycerol, 5 mM $MgCl_2$, 5 mM β-mercaptoethanol) using a PD-10 desalting column (SephadexTM G-25, Pharmacia) and the protein was stored at −80 °C.

***A. terreus* Aristolochene Synthase.** Individual strains of *E. coli* BL21(DE3)pLysS/pET11rASa and derivatives harboring the wild-type and mutant plasmids of *A. terreus* aristolochene synthase were grown overnight in 10 mL of LB media containing 100 μg/mL carbenicillin at 37 °C. The overnight seed culture was used to inoculate 1 L of pre-warmed (30 °C) LB-carbenicillin (100 μg/mL) and the cells were grown until the OD_{600} reached 1.0. Protein expression was then induced with 1 mM IPTG. After 6 h of incubation the cells were harvested by centrifugation (6000 × *g*, 30 min, 4 °C). The pellet was then re-suspended in 50 mL of MEG buffer (20 mM Mes pH 6.5, 2 mM EDTA, 10% glycerol, 5 mM 2-mercaptoethanol) and recentrifuged (6000 × *g*, 30 min, 4 °C) to remove any remaining LB medium. The cells were resuspended in 50 mL of MEG buffer and broken by sonication (three cycles of 10 min each, 50% duty cycle and 30% power range) in an ice water bath. The crude cell lysate was centrifuged (17 000 × *g*, 30 min, 4 °C) and the supernatant, containing soluble aristolochene synthase was collected. The subsequent purification of the *A. terreus* aristolochene synthase was based on the previously published procedure for the wild-type protein.[5] Fractions containing pure enzyme were located by SDS-PAGE and combined. The solution was concentrated to 0.5 mL using an Amicon ultrafiltration apparatus equipped with an YM-10 filter, the buffer was changed to protein storage buffer (20 mM Hepes pH 8.0, 5 mM $MgCl_2$ and 10% glycerol) using a PD-10 desalting column and the protein was stored at −80 °C. Using the above expression procedure, the *A. terreus* mutant *AT*-N219D was obtained exclusively as inclusion bodies despite the use of lower induction temperatures, lower IPTG concentrations and longer induction time. Cells were therefore suspended in 50 mL of cell lysis buffer (MEG buffer) and sonicated. The lysate was centrifuged (6000 × *g* for 30 min at 4 °C) and the pellet, containing the insoluble inclusion bodies, was resuspended in 200 mL of MEG buffer. The inclusion bodies were solubilized and the protein was purified following the same method used for the *P. roqueforti* enzymes[11] except that MEG buffer was utilized for the solubilization and purification. The fractions containing the protein were combined and concentrated using a centriprep YM-30 centrifugal filter to a final volume of 2.5 mL, the buffer was changed to protein storage buffer using a PD-10 desalting column, and the protein was stored at −80 °C.

(30) Sambrook, J.; Fritsch, E. F.; Maniatis, T. *Molecular Cloning: a Laboratory Manual*; Cold Spring Harbor Laboratory Press: Cold Spring Harbor, NY, 1989. *Current Protocols in Molecular Biology*, *CD-ROM*; Wiley: New York, 1999.
(31) Bradford, M. *Anal. Biochem.* **1976**, *72*, 248−254.
(32) Schwede, T.; Kopp, J.; Guex, N.; Peitsch, M. C. *Nucleic Acids Res.* **2003**, *31*, 3381−3385. Guex, N.; Peitsch, M. C. *Electrophoresis* **1997**, *18*, 2714−2723. Peitsch, M. C. *Bio/Technology* **1995**, *13*, 658−660.

Aristolochene Synthase Assay and Kinetics. The activity of the *P. roqueforti* mutants was assayed by a modification of the procedure previously described for wild-type aristolochene synthase.[5] To determine the concentration dependence of activity for each mutant, increasing concentrations of protein (2 nM to 510 nM) were incubated with FPP (**1**) at constant concentrations (2−20 μM) of FPP (**1**) in Buffer T. The specific activity of the FPP was adjusted by mixing unlabeled FPP with [1-^{3}H]FPP (16 Ci/mmol) to a value of 40−170 μCi/μmol. Incubations were initiated by addition of cyclase (30 μL containing 40 ng to 10 μg of protein) to 500 μL of pre-warmed (30 °C) Buffer H (20 mM Hepes pH 8.0, 5 mM $MgCl_2$, 5 mM 2-mercaptoethanol) containing FPP. After 10 min the reaction was quenched by addition of 200 μL of 100 mM EDTA (pH 7.5) and the mixture was transferred to an ice bath. Hexane (1 mL) was added, the mixture was vortexed for 20 s, and the organic extract was withdrawn and passed through a 2-cm silica gel column, directly into a scintillation vial containing 10 mL of scintillation cocktail. Another extraction was performed with 500 μL of hexane, followed by a final wash of 900 μL hexane. The hexane elutable activity was measured by scintillation counting. A blank control was run without enzyme to correct for the nonenzymatic solvolysis of FPP. Each assay was conducted in triplicate under the same experimental conditions.

Kinetic assays of aristolochene synthase mutants were carried out in the same manner. Each assay used a constant protein concentration (2.6−400 nM) and varying concentrations of [1-^{3}H]FPP (**1**) (specific activity 20−800 μCi/μmol). The concentrations of [1-^{3}H]FPP were chosen so as to bracket the experimental K_m for each mutant. The enzyme concentration was set within the range in which the activity of the mutant had been found to be a linear function of protein concentration and such that the percentage conversion of FPP to products was less than 10% over the 10 min assay period. Steady-state kinetic parameters were determined by direct fitting of the data to the Michaelis−Menten equation by nonlinear least squares regression using the commercial Kaleidagraph package (Synergy Software).

For wild-type and mutant *A. terreus* aristolochene synthase, activity assays were conducted in Buffer H following the procedure described above, using 2−10 μM FPP (**1**) (specific activity 50−150 μCi/μmol) and fixed concentrations of 0.9−410 nM protein. Kinetic assays of *A. terreus* aristolochene synthase mutants were carried out as described above. Each assay was conducted in Buffer H and used a constant protein concentration (1−100 nM) and varying concentrations of [1-^{3}H]FPP (**1**) (specific activity 150−500 μCi/μmol).

Product Analysis. For preparative-scale incubations, purified wild-type or mutant *P. roqueforti* aristolochene synthase (80−510 nM) was incubated with FPP (**1**) (25−50 μM) in Buffer T at 30 °C for 3 h. Preparative-scale incubations of *A. terreus* wild-type and mutant aristolochene synthases were carried out in the same manner using Buffer H. The concentration of each mutant was the maximum value tested at which each protein retained concentration-independent specific activity. The volume of buffer used in each incubation was adjusted for the maximum concentration of protein so as to produce enough product for detection by GC−MS (Table 3). The aqueous layer was overlaid with HPLC-grade pentane (10% by vol). The hydrocarbon products were extracted twice with pentane (10% by vol). The extracts were combined, concentrated to 5 mL under reduced pressure at 0 °C, and passed through an alumina column (3 cm, packed in a Pasteur pipet) overlaid with sodium sulfate. The organic layer was then concentrated to 200 μL under reduced pressure at 0 °C. The concentrate was analyzed by GC−MS using either an Optima 1701 or chiral FS-hydrodex-β-6TBDM capillary GC column. With the Optima 1701 column, the injection port temperature was either at 150 or 250 °C with an initial column temperature 45 °C for 4 min, followed by a gradient of 6 °C/min to a maximum of 220 °C. Under these conditions (+)-aristolochene (**4**), (−)-valencene (**5**) and (−)-germacrene (**2**) and (+)-β-elemene (**7**) eluted typically at 15.47, 15.61, 15.71 and 13.51 min, respectively. For the FS-hydrodex β-6TBDM column, splitless injections were carried out using an injection port temperature of 150 or 250 °C with an initial column temperature 45 °C for 4 min, followed by a gradient of 2 °C/min to a maximum of 180 °C.[16] Under these conditions (+)-aristolochene (**4**), (−)-valencene (**5**), (*S*)-(−)-germacrene A (**2**) and (+)-β-elemene (**7**) typically eluted at 51.57, 51.04, 53.33, and 45.41 min, respectively. Mass spectra data were compared to those in the NIST98 mass spectral database and to those obtained from authentic standards.

Table 3. Preparative-Scale Incubation Conditions

protein	buffer T (ml)	protein (nM)	FPP (μM)
P. roqueforti WT[a]	20	80	25
D115E	20	160	25
D116E	20	410	25
D116N	20	510	25
E119D	20	260	25
E119Q	20	510	25
N244D	160	510	50
S248A	20	410	50
E252D	20	410	50
E252Q	160	510	50
Y92F	170	50	25
A. terreus WT	60[b]	100	25
AT-N219D	170[b]	410	25
AT-E227D	150[b]	410	25

[a] WT, wild-type. [b] Buffer H.

Acknowledgment. This research was supported by an NIH Merit Award (GM30301) to D.E.C.

Supporting Information Available: GC-MS analysis of E252Q product. This material is available free of charge via the Internet at http://pubs.acs.org.

JA0499593